科学通报
进 展
《中国科学》杂志社
SCIENCE CHINA PRESS

功能化富勒烯在锡基钙钛矿太阳能电池中的研究进展

孙超, 邢益铭, 张蕙, 陈珊珊, 田成波*, 魏展画*

华侨大学材料科学与工程学院, 发光材料与信息显示研究院, 光电材料与先进制造厦门重点实验室, 厦门 361021

* 联系人, E-mail: cbtian@hqu.edu.cn; weizhanhua@hqu.edu.cn

2024-12-23 收稿, 2025-02-18 修回, 2025-02-18 接受, 2025-02-26 网络版发表
国家自然科学基金(52472201)资助

摘要 锡基钙钛矿因其低毒性和高理论光电转化效率, 受到了科研界的广泛关注. 然而, Sn^{2+}易被氧化、结晶速度难以调控, 以及与常用电子传输材料能级失配等问题限制了锡基钙钛矿电池的进一步发展, 使其最高效率与理论效率间仍存在较大差距. 富勒烯因其优异的电荷传输性能和缺陷钝化能力被认为是解决锡基钙钛矿太阳能电池问题的关键材料之一, 近年来的相关研究也取得了显著的成效. 因此, 本文首先分析了锡基钙钛矿的问题及其成因, 随后立足于富勒烯在器件中的具体用途, 对不同功能化富勒烯材料用于改善锡基钙钛矿器件性能的相关研究进行了分类讨论和总结. 最后, 鉴于锡基钙钛矿电池的研究现状, 对未来富勒烯材料的研究重点进行了展望.

关键词 锡基钙钛矿太阳能电池, 功能化富勒烯, 能级匹配, 界面钝化, 结晶调控

近年来, 得益于钙钛矿材料光吸收系数高、带隙可调、激子结合能低以及可溶液制备等一系列优点[1~5], 有机-无机卤化物钙钛矿太阳能电池被广泛研究并迅速发展. 在短短十几年内, 钙钛矿太阳能电池最高光电转换效率已从3.8%迅速提升至26.7% (https://www.nrel.gov/pv/cell-efficiency.html)[6,7], 成为第三代新型光伏技术的代表之一. 然而, 目前高效钙钛矿太阳能电池的研究都是基于铅基钙钛矿[8,9], 这种含铅的材料一旦投入商业化应用, 其生产、运输、储存和使用等诸多过程均存在泄漏的风险, 进而造成生物危害和环境污染问题[10~12]. 为此, 研究者们通过将ABX_3型钙钛矿结构中的B位Pb^{2+}替换为其他二价金属阳离子(图1(a)), 开发出多种低毒或无毒的非铅钙钛矿材料[13~18]. 值得注意的是, 锡元素与铅元素处于同一主族, 具有相似的原子构型和离子半径, 使得锡基钙钛矿具有许多与铅基钙钛矿相似的光电性能, 包括高载流子迁移率和高光吸收系数等[19~21]. 此外, 锡基钙钛矿的带隙更窄, 接近单节太阳能电池的理论最佳带隙(约为1.34 eV)[22~25], 使得其理论效率可达到33%以上(图1(b))[26,27].

然而, 锡基钙钛矿电池目前的最高光电转化效率仅为15.7%[28], 不仅远低于其理论效率, 也不及铅基钙钛矿的最高效率. 从电子构型的角度看, 如图1(c)所示, 锡原子与铅原子相似, 其最外层的5*s*轨道上同样存在4个电子. 然而, Sn原子失去两个电子后形成的Sn^{2+}相较于Pb^{2+}具有更强的Lewis酸性, 因而更易于与有机铵盐迅速反应形成钙钛矿晶体, 这导致锡基钙钛矿的结晶速度更快, 难以形成均匀致密的薄膜[29~31]. 另一方面, 由于缺乏镧系收缩带来的$6s^2$惰性电子对效应, Sn^{2+}相较于Pb^{2+}更容易被氧化为Sn^{4+}, 不仅会显著影响器件性能, 产生的Sn^{4+}还可能会催化该氧化过程, 导致锡基钙钛矿的自催化分解[32~34].

从能级的角度来看, 锡基钙钛矿的能带结构主要由Sn和X位离子主导, A位离子对其影响相对较小. 以$MASnI_3$为例(图1(d)), 其导带底(conduction band minimum, CBM)主要由Sn-5*p*轨道反键与极少量的I-5*p*轨道

引用格式: 孙超, 邢益铭, 张蕙, 等. 功能化富勒烯在锡基钙钛矿太阳能电池中的研究进展. 科学通报
Sun C, Xing Y, Zhang H, et al. Research progress on functionalized fullerenes in tin-based perovskite cells (in Chinese). Chin Sci Bull, doi: 10.1360/TB-2024-1360

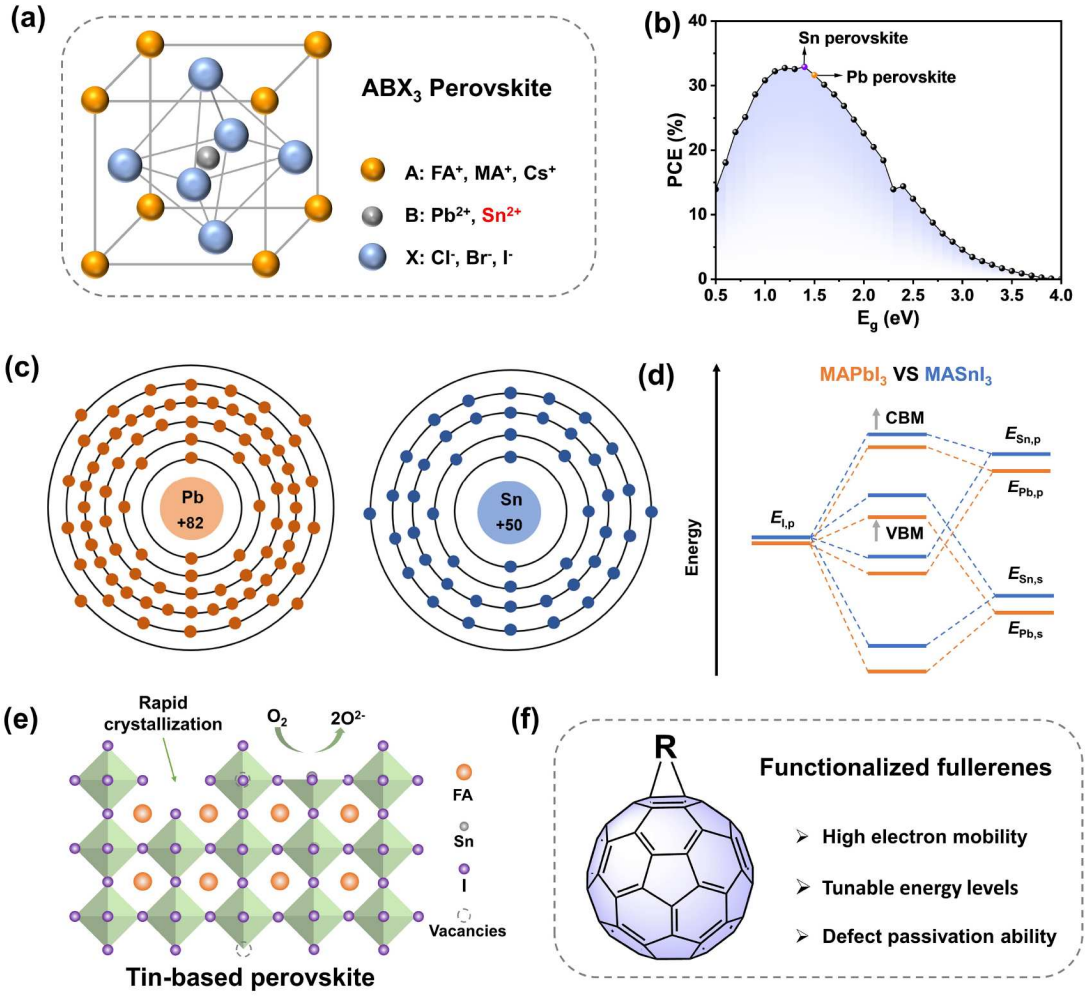

图 1 (网络版彩色)锡基钙钛矿与富勒烯的结构与性能. (a) ABX_3型钙钛矿结构示意图; (b) 单节电池的Shockley-Queisser效率极限图[27]; (c) 锡原子与铅原子的电子构型对比示意图; (d) $MAPbI_3$与$MASnI_3$的能级对比; (e) 锡基钙钛矿的晶体缺陷及空位示意图; (f) 功能化富勒烯的结构与优势

Figure 1 (Color online) Structure and properties of tin-based perovskites and fullerenes. (a) Schematic diagram of the ABX_3 perovskite structure. (b) Shockley-Queisser efficiency limit graph for single-junction solar cells[27]. (c) Schematic comparison of the electronic configurations of tin and lead atoms; (d) Energy level comparison between $MAPbI_3$ and $MASnI_3$. (e) Schematic diagram of crystal defects and vacancies in tin-based perovskite. (f) The structure and advantages of functionalized fullerenes

反键耦合构成, 而其价带顶(valence band maximum, VBM)则主要由Sn-5*s*轨道反键与I-5*p*轨道反键耦合形成[32,35]. 由于其Sn-5*p*轨道和Sn-5*s*轨道的能级均高于$MAPbI_3$中的Pb-6*p*轨道和Pb-6*s*轨道, 因此锡基钙钛矿的CBM和VBM均高于铅基钙钛矿[36]. 这也使得Sn-I键相较Pb-I更容易断裂形成锡空位缺陷(图1(e))[37], 进而导致锡基钙钛矿出现严重的p型自掺杂. 由此引发的背景载流子浓度甚至可高达10^{18} cm^{-3}以上[34,38], 造成器件内严重的载流子复合. 同时, 锡基钙钛矿更高的CBM与常用的富勒烯基电子传输材料的能级不匹配, 进一步加剧了界面处的非辐射复合, 造成严重的开路电压损失.

富勒烯是由sp^2杂化碳原子组成的封闭笼状碳簇分子(图1(f)), 其不仅具备高电子迁移率和缺陷钝化性能[39,40], 还能通过打开具有双键特性的[6,6]键加成多种不同的功能基团, 以获得具备各种特定功能的富勒烯衍生物材料, 因此被广泛用于锡基钙钛矿电池领域以改善上述问题. 基于此, 本文综述了近年来新型功能化富勒烯衍生物材料用于改善锡基钙钛矿太阳能电池性能方面的研究进展, 并根据其应用方式进行了分类讨论. 最后, 总结了该领域的研究现状, 并展望了未来功能化富勒烯材料的开发与设计方向.

1 功能化富勒烯用于改善TPSCs性能

1.1 富勒烯体相掺杂

为了解决锡基钙钛矿中Sn^{2+}易被氧化及其结晶过程难以调控的问题，大量添加剂工程相关的工作被报道. 这些研究主要通过在锡基钙钛矿前驱体溶液中引入具有氧化膦基、羧基和氨基等配位基团有机分子添加剂与钙钛矿组分产生相互作用，从而调控锡基钙钛矿的结晶并抑制其氧化，以获得高质量的锡基钙钛矿薄膜[41~47].

然而, 这些有机钝化剂分子大多是绝缘的, 会阻碍电荷传输, 并限制器件性能的进一步提高. 鉴于富勒烯材料良好的导电性，一系列带有合适功能基团的功能化富勒烯衍生物添加剂被开发并引入锡基钙钛矿电池领域. 研究初期, 为实现与锡基钙钛矿更强的相互作用, 带有多个作用基团的富勒烯添加剂受到了广泛关注, 例如, 2022年, Chen等人[48]设计合成了三种多功能离子富勒烯衍生物(命名为C_{60}-RNH_3-X; X=Cl、Br或I)，并将其用作锡基钙钛矿体相添加剂研究结果表明，这些大尺寸的球形离子富勒烯卤化物添加剂因无法进入钙钛矿晶格, 而主要位于其晶界, 不仅可以成为钙钛矿晶粒间的载流子传输介质(图2(a))，还可以通过与Sn^{2+}离子相互作用钝化晶界缺陷并抑制Sn^{2+}氧化. 此外，分子中的卤素阴离子可以减缓反溶剂滴加过程中的钙钛矿晶体的结晶速率，并填充X位缺陷，从而获得了高质量的锡基钙钛矿薄膜. 最终，基于C_{60}-RNH_3-Br的器件实现了最高为11.7%的光电转化效率. 同年, Chen等人[49]合成并使用了一种含氯的富勒烯添加剂分子，$C_{60}Cl_6$. 研究结果显示, $C_{60}Cl_6$的六个氯可与钙钛矿组分产生化学相互作用以延缓了前驱体向钙钛矿晶体的转化过程, 从而实现了高质量的锡基钙钛矿薄膜. 同时，如图2(b)所示，位于表面和晶界的$C_{60}Cl_6$不仅可以钝化缺陷，还可以缝合晶界以抑制外界的水氧对钙钛矿薄膜的侵蚀, 特别是会抑制Sn^{2+}被氧化为Sn^{4+}. 最终, 基于$C_{60}Cl_6$的器件相比对照器件，光电转化效率由10.03%提高至13.30%, 稳定性也明显增强.

带有多个功能基团的富勒烯添加剂可能会限制钙钛矿薄膜中的电荷传输, 因此, 一些单取代富勒烯添加剂也在近年来相继被开发及使用. 2023年, Choi等人[50]设计并使用了一种具有三乙二醇单乙醚侧链的吡咯烷富勒烯(PTEG-1). 研究发现, PTEG-1不仅可以通过碳笼与I结合以抑制I_3^-的形成，其醚基团还可以与Sn^{2+}配位以改善锡基钙钛矿陷阱态引起的非辐射复合(图2(c)), 因此获得了光滑无孔的高质量钙钛矿薄膜. 最终, 基于PTEG-1的器件实现了8.78%的最高光电转化效率. 同时, 封装后的器件在空气中光照1000 h后, 仍保留了约65%的初始效率. 2024年, Chen等人[51]合成并使用了两种吡咯烷富勒烯添加剂分子，CPPF和TPPF. 研究结果显示, CPPF和TPPF的空间构型会极大地影响了它们的电子密度分布和与钙钛矿组分的相互作用. 与CPPF相比，TPPF的两个吡啶官能团之间空间距离更大可以有效地增加其与不同钙钛矿胶体相互作用的概率，从而减少钙钛矿薄膜制备过程中的成核数量，因此获得了具有更高质量的锡基钙钛矿薄膜. 此外，TPPF的引入还会提升钙钛矿薄膜的能级，改善与电子传输层的能级匹配. 最终，如图2(d)所示，基于TPPF的器件的最高光电转化效率达到了15.38%(认证效率为15.14%). 同时，由于TPPF引入后钙钛矿薄膜质量的提高和抗超氧阴离子的增强，未封装的器件在储存3000 h和连续照射500 h后分别保持了其初始效率的99%和93%. 除此之外，可原位交联的富勒烯添加剂也被研究用于锡基钙钛矿以延迟其结晶过程，优化晶格匹配并降低薄膜中的机械应力，从而提高锡基器件的效率. 例如Hou等人[52]合成了一种硫辛酸官能化的富勒烯吡咯烷碘化物(FTAI)，并将其掺入锡基钙钛矿中. FTAI上的C=O和S-S均可以与Sn^{2+}配位，调节锡基钙钛矿的结晶速率和薄膜质量. 同时，FTAI在钙钛矿退火过程中(70℃)可以原位交联, 且不会限制钙钛矿晶粒的生长. 由于富勒烯材料的固有导电性确保了即使在交联后，也不会影响相应薄膜中的载流子传输，同时还会使钙钛矿晶界处富含交联FTAI，进而显著提高了钙钛矿薄膜的抗弯折性能. 因此，基于FTAI的刚性装置实现了14.91%的最高效率，远高于对照器件(12.00%). 相应的，柔性锡基钙钛矿电池的效率也获得了12.35%的纪录效率，并表现出优异的弯曲稳定性. 在曲率半径为5 mm的情况下弯曲10000次后，该器件的效率仍保持了初始效率的90%左右. 上述研究结果充分证明了开发有效的富勒烯体相添加剂以获得高质量的钙钛矿薄膜，对于实现高效稳定的锡基钙钛矿电池具有重要意义.

1.2 富勒烯界面层

由于n-i-p型器件中空穴传输材料的酸性导电掺杂剂会锡基钙钛矿薄膜降解，且锡基钙钛矿本身存在p型自掺杂问题，因此锡基钙钛矿电池通常采用p-i-n型器

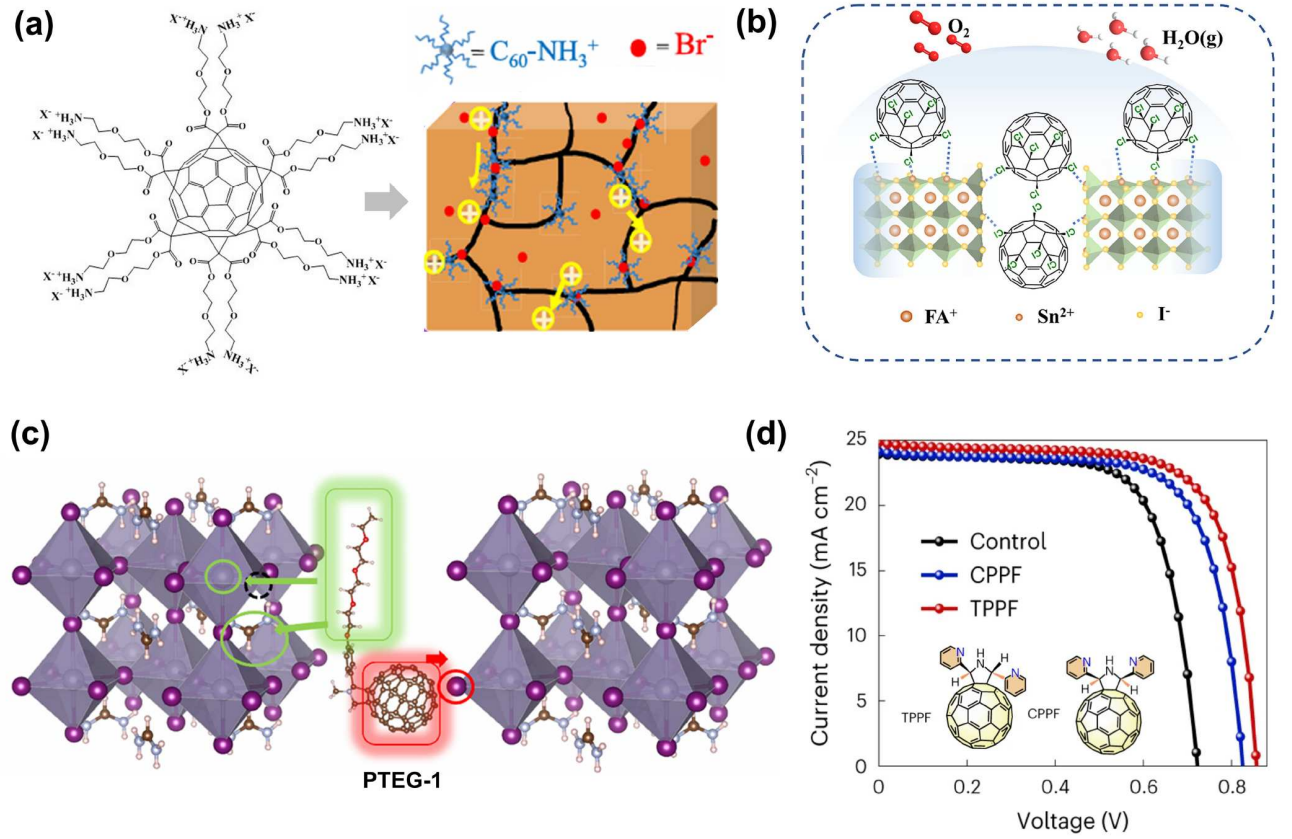

图 2 (网络版彩色)富勒烯体相掺杂剂. (a) C_{60}-RNH_3-X的分子结构(X=Cl、Br或I)及其改善钙钛矿晶界电荷传输的示意图[48]; (b) $C_{60}Cl_6$提高器件性能的原理示意图[49]; (c) PTEG-1与锡基钙钛矿相互作用的示意图[50]; (d) CPPF和TPPF的结构及其器件的*J-V*曲线[51]

Figure 2 (Color online) Fullerene bulk additives. (a) Molecular structure of C_{60}-RNH_3-X (X=Cl, Br, or I) and the schematic diagram of improvement in charge transport at perovskite grain boundaries[48]. (b) Schematic diagram of the $C_{60}Cl_6$-assisted strategy for device performance enhancement[49]. (c) Schematic diagram of the interaction between PTEG-1 and tin-based perovskite[50]. (d) Molecular structure of CPPF and TPPF and the *J-V* curves of their devices[51]

件结构. 然而, 常用的富勒烯基电子传输材料, 如C_{60}和PCBM等, 存在与锡基钙钛矿能级失配和钝化作用较弱等问题, 导致器件界面处产生高能量损失和深陷阱态缺陷[53~55]. 因此, 优化锡基钙钛矿/电子传输层界面对提高锡基钙钛矿电池性能具有重要意义. 然而, 常用于铅基钙钛矿电池界面钝化的有机铵盐分子, 其极性溶剂会溶解锡基钙钛矿薄膜, 并不适用于锡基钙钛矿电池. 而富勒烯基修饰分子的溶剂大多为甲苯、氯苯等不会破坏锡基钙钛矿的有机溶剂, 且富勒烯本身具有非常优异的缺陷钝化能力, 因此被认为是非常有潜力的界面修饰材料.

2022年, Li等人[56]开发了一种吡啶官能化富勒烯衍生物C_{60}-BPy(图3(a)), 用以来修饰钙钛矿/ETL界面, 解决缺陷、能量无序和能级失配的问题. 研究结果证明, C_{60}-BPy可以通过吡啶基团和Sn^{2+}离子之间的配位相互作用强烈锚定在钙钛矿表面, 从而不仅实现了锡钙钛矿薄膜内陷阱态的钝化, 还改善了界面能级匹配以减少非辐射复合. 因此, 基于C_{60}-BPy的器件实现了14.14%的最高光电转化效率以及可忽略的迟滞. 此外, C_{60}-BPy所带来的界面钝化和载流子输运性能的提升, 也显著增强了器件的稳定性. 经测试, 基于C_{60}-BPy的未封装器件在太阳光连续照射1000 h后, 仍能够保持初始效率的95%以上.

由于界面层通常较薄, 电子隧穿效应的存在使得其导电性对于器件电荷传输的影响较小. 因此, 带有多个基团的富勒烯分子也被用于进一步改善锡基钙钛矿/电子传输层界面的性能. 2024年, Sun等人[57]精准合成了四种分别带有3、4、5和6个丙二酸二乙酯基团的多齿富勒烯分子(FM3、FM4、FM5和FM6)并用于锡基钙钛矿电池的界面修饰. 研究结果显示, 富勒烯功能基

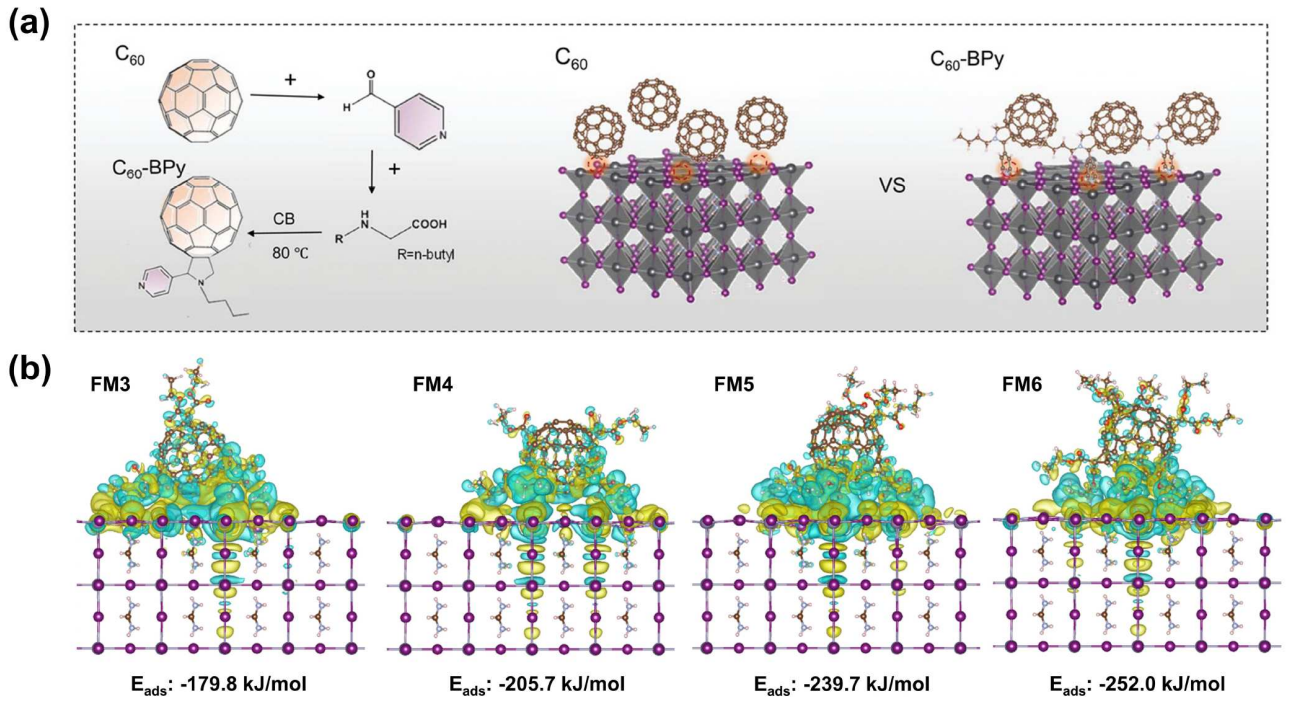

图 3 (网络版彩色)富勒烯界面层. (a) C_{60}-BPy的合成路线以及钙钛矿和C_{60}(或C_{60}-BPy)之间界面相互作用的示意图[56]; (b) 多齿富勒烯在钙钛矿薄膜上的计算结构模型和吸附能(E_{ads})[57]

Figure 3 (Color online) Fullerene interfacial layers. (a) Synthetic Routes of C_{60}-BPy and the schematic illustration of the interfacial interactions between the perovskite and C_{60} (or C_{60}-BPy)[56]; (b) calculated structural models and absorption energies (E_{ads}) of multidentate fullerenes onto the perovskite film[57]

团数量的增加会导致LUMO能级变浅以及界面化学相互作用的增强(图3(b)). 其中, FM5表现出合适的能级和与钙钛矿的强配位相互作用, 可以有效地改善电子提取并钝化界面缺陷. 此外, FM5独特的分子结构使暴露的碳笼在其基团与钙钛矿相互作用后与可以上层富勒烯的碳笼紧密堆叠, 从而实现更有效的电荷转移并保护钙钛矿免受水分和氧气的损害. 最终, 基于FM5的器件实现了15.05%的冠军效率, 显著超过了基于PCBM (11.77%)、FM3(13.54%)、FM4(14.34%)和FM6 (13.75%)的器件. 此外, 基于FM5的器件表现出优异的稳定性, 即使在空气暴露300 h后, 也能保持其初始效率的90%以上.

1.3 富勒烯电子传输层

合成具有更高LUMO能级和更强配位相互作用的富勒烯材料并将其直接用作锡基钙钛矿电池的电子传输层, 也是解决锡基钙钛矿与C_{60}、PCBM等能级失配问题的有效手段之一. 因此, 2022年, Wu等人[58]参考有机太阳能电池中提高富勒烯LUMO能级的策略, 通过在富勒烯碳笼上引入给电子基团, 设计合成了两种富勒烯衍生物C_{60}-MP和C_{60}-ETPA, 并用作锡基钙钛矿电池的电子传输层. 研究结果证明, 引入的二甲氧基苯, 三苯胺基团和烷基链降低了富勒烯的电子亲和力, 导致其LUMO能级比PCBM的能级更高. 此外, 更匹配的能级提供了有效的载流子传输并抑制了电荷复合. 最终, 如图4(a)所示, 基于C_{60}-ETPA的器件实现了0.76 V的开路电压和超过10%的光电转换效率, 显著高于对照器件的0.63 V和8.25%.

经过功能基团优化后的单取代富勒烯电子传输材料, 虽然有效改善了能级匹配, 但仍存在界面钝化效果较弱的问题. 为此, 与锡基钙钛矿具有更强相互作用的一系列二取代富勒烯电子传输材料也被开发及使用. 2020年, Jiang等人[59]引入茚-C_{60}双加成物(ICBA)作为锡基钙钛矿电池的电子传输层, 以取代通常使用的PCBM(图4(b)). ICBA具有较浅的能级(图4(b)), 可实现更高的开路电压, 并抑制碘化物的远程掺杂, 从而减少界面载流子复合. 因此, 使用ICBA将器件的开路电压成功提高到0.94 V, 明显高于使用PCBM作为电子传输层的器件(0.6 V). 基于ICBA的器件也获得了12.4%的效率以及可忽略的迟滞(图4(c)). 此外, 该器件展现出

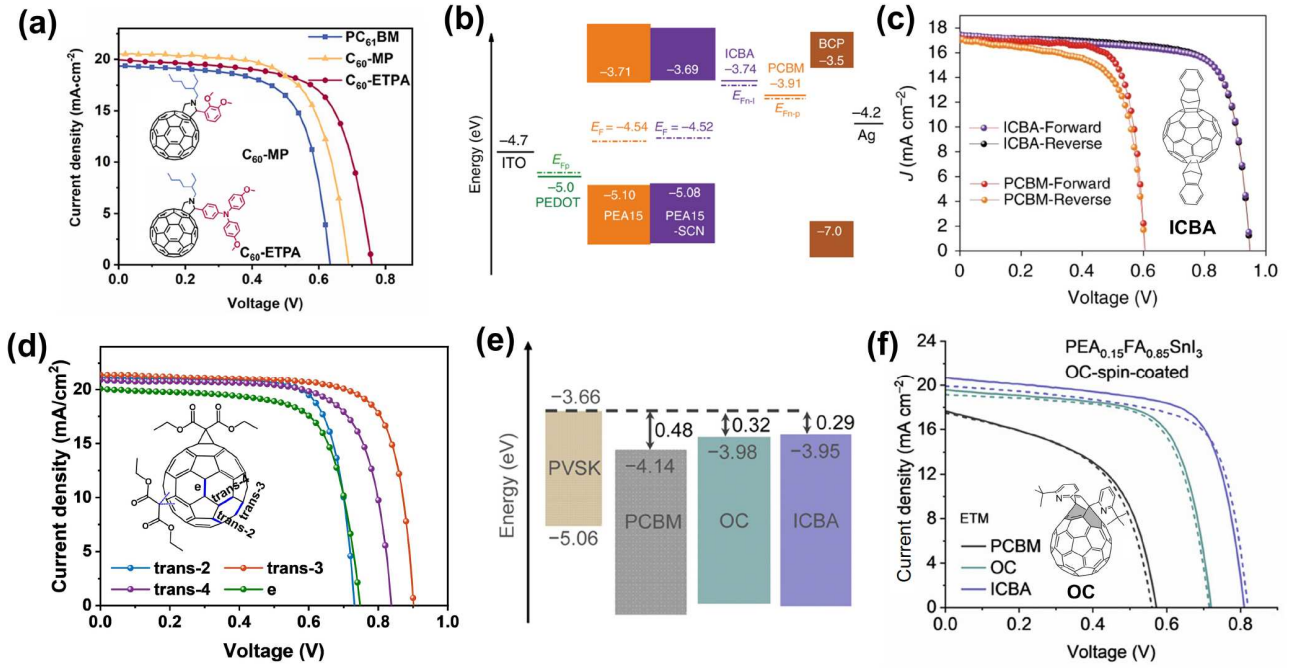

图 4 (网络版彩色)富勒烯电子传输层. (a) C_{60}-MP、C_{60}-ETPA的分子结构及其器件和基于PCBM的器件的*J-V*曲线[58]; (b) ICBA、PCBM与锡基钙钛矿等的能级排列示意图; (c) 基于ICBA和 PCBM的最佳器件的*J-V*曲线[59]; (d) 基于不同二取代富勒烯异构体的*J-V*曲线[63]; (e) 钙钛矿和PCBM、OC和ICBA薄膜的能级图; (f) 基于PCBM、OC和ICBA的最佳器件的*J-V*曲线[64]

Figure 4 (Color online) Fullerene electron transport layers. (a) The molecular structures of C_{60}-MP and C_{60}-ETPA, as well as the *J-V* curves of their devices and PCBM-based devices[58]. (b) Schematic diagram of energy level arrangement for ICBA, PCBM, and tin-based perovskite. (c) *J-V* curve of the champion device based on ICBA and PCBM[59]. (d) Characteristic *J-V* curves of the TPSCs based on different ETLs[63]. (e) Energy level diagrams of perovskite and PCBM, OC, and ICBA films; (f) *J-V* curves of optimal devices based on PCBM, OC, and ICBA[65]

优异的长期储存稳定性, 在惰性气体环境中存放3800 h后仍保持初始效率的90%. 在该工作的基础上, 大量使用ICBA或其他二取代富勒烯作为电子传输层并对器件进一步优化的工作相继被报道[60~62], Shi等人[28]也于2024年成功实现了15.7%的锡基钙钛矿电池纪录效率, 证明了二取代富勒烯在改善锡基钙钛矿的能级匹配问题上的巨大潜力.

然而, 二取代富勒烯通常为多种位置异构体构成的混合物, 不仅会因不利堆积导致能量无序, 还可能因不同批次间各异构体含量不同导致实验重现性差. 为此, 2022年, Sun等人[63]分离提纯了丙二酸二乙酯-C_{60}双加成物(DCBA)的四个异构体(trans-2、trans-3、trans-4和e), 并将其用于锡基钙钛矿电池以探究不同二取代富勒烯异构体对于器件性能的影响规律. 通过单晶X射线衍射明确地确定了四种异构体的化学结构并系统地探讨了两个功能基团的相对位置对它们的能级、分子堆积模式、电子迁移率和界面相互作用的影响. 值得注意的是, 如图4(d)所示, 由于LUMO能级较浅, 分子堆积更有利, 界面相互作用增强, 基于trans-3的器件获得了14.58%的最高效率(认证效率为14.30%), 不仅高于基于trans-2(11.69%)、trans-4(12.59%)和e(10.55%)的器件效率, 也高于基于异构体混合物DCBA(10.28%)的器件效率. 其阐明的结构-性质关系可以指导二取代富勒烯的设计和应用, 以助力未来实现更高效的锡基钙钛矿电池. 在该工作基础上, 考虑到这些异构体的分离纯化耗时耗力, 他们还采用了一种空间限域的合成策略[64], 精准合成了具有特定结构的二取代富勒烯分子C_{60}BB和C_{70}BB, 并通过溶剂工程进一步调控了其作为电子传输层的电荷传输性能, 最终分别实现了光电转化效率为14.51%和14.28%的锡基钙钛矿器件.

此外, Liu等人[65]使用了一种无异构体的开笼二取代富勒烯(OC)作为锡基钙钛矿电池的电子传输层以解决锡基钙钛矿电池的能级失配问题. 研究表明, OC在保留了C_{60}的完整60π系统的基础上, 还具有两个[5,6]开放结构, 从而实现了与锡基钙钛矿匹配的能级(图4(e)). 因此, 如图4(f)所示, 使用OC作为电子传输层的锡基钙钛矿器件实现了0.72 V的开路电压和9.6%的光电转化效率. 同时, 由于OC出色的热稳定性, 可以通过真

空热蒸镀工艺进行薄膜和器件制备，以实现灵活可调的膜厚和器件性能的可重复性. 最终，基于真空蒸镀OC的器件也实现了7.6%的光电转化效率，为开发具备合适能级的锡基钙钛矿电池电子传输材料提供了新的思路.

2 总结与展望

本文根据体相掺杂、界面修饰以及电子传输等使用方式，对基于功能化富勒烯材料改善锡基钙钛矿太阳能电池性能的研究工作进行了归纳总结. 针对锡基钙钛矿的Sn^{2+}易被氧化、结晶过快不易调控和与常用电子传输材料能级失配等问题，各种功能化富勒烯材料的引入取得了显著的效果，并实现了15.7%的最高光电转化效率. 然而，与主流的铅基钙钛矿电池间显著的性能差距仍需要在各类功能化富勒烯材料的设计，开发及使用等方面进行更深入的探究. 为此，我们认为未来研究可重点关注以下方向:

(1) 富勒烯界面修饰: 使用有机卤化物铵盐进行钙钛矿表面钝化已成为铅基钙钛矿电池的基础工艺之一，但由于这些铵盐所使用的溶剂会溶剂锡基钙钛矿，因此无法直接推广用于锡基钙钛矿电池. 而通常使用甲苯、氯苯等作为溶剂的功能化富勒烯材料，不仅不会破坏锡基钙钛矿，还可以通过优化取代基的结构和数量，实现高效的钝化作用，从而抑制非辐射复合以实现高开路电压.

(2) 基于富勒烯进行能级调控: 锡基钙钛矿与常用的电子传输材料间的能级失配也是造成器件较大开路电压损失的重要因素之一. 因此，在设计合成具有更强钝化作用的功能化富勒烯材料时，还需兼顾其能级是否合适. 从而可以通过体相掺杂、界面修饰或直接作为电子传输材料等方式引入锡基钙钛矿器件，以改善其能级失配问题，进一步提升器件性能.

(3) 功能化富勒烯材料的联用: 目前已报道的基于功能化富勒烯材料优化锡基钙钛矿电池性能的工作，通常通过比较单一富勒烯材料引入前后的性能变化，以明确材料本身对于器件性能的具体影响，而对照组器件本身采用的器件结构则较为基础. 为了进一步实现锡基钙钛矿电池的效率突破，未来可能需要在器件的不同功能层联用多种功能化富勒烯材料以协同解决锡基钙钛矿的各类问题.

锡基钙钛矿电池的高理论效率和低毒性决定了其高商业价值，随着功能化富勒烯材料的持续创新和优化，锡基钙钛矿电池有望实现性能突破，在光伏发电领域发挥出其全部的潜力.

参考文献

1 Sun S, Salim T, Mathews N, et al. The origin of high efficiency in low-temperature solution-processable bilayer organometal halide hybrid solar cells. Energy Environ Sci, 2014, 7: 399–407
2 Park N G. Perovskite solar cells: an emerging photovoltaic technology. Mater Today, 2015, 18: 65–72
3 Jung H S, Park N. Perovskite solar cells: from materials to devices. Small, 2015, 11: 10–25
4 Stranks S D, Eperon G E, Grancini G, et al. Electron-hole diffusion lengths exceeding 1 micrometer in an organometal trihalide perovskite absorber. Science, 2013, 342: 341–344
5 Heo J H, Im S H, Noh J H, et al. Efficient inorganic–organic hybrid heterojunction solar cells containing perovskite compound and polymeric hole conductors. Nat Photon, 2013, 7: 486–491
6 Kojima A, Teshima K, Shirai Y, et al. Organometal halide perovskites as visible-light sensitizers for photovoltaic cells. J Am Chem Soc, 2009, 131: 6050–6051
7 Green M A, Dunlop E D, Yoshita M, et al. Solar cell efficiency tables (Version 64). Prog Photovoltaics, 2024, 32: 425–441
8 Liang Z, Zhang Y, Xu H, et al. Homogenizing out-of-plane cation composition in perovskite solar cells. Nature, 2023, 624: 557–563
9 Zhou J, Tan L, Liu Y, et al. Highly efficient and stable perovskite solar cells via a multifunctional hole transporting material. Joule, 2024, 8: 1691–1706
10 Chen C H, Cheng S N, Cheng L, et al. Toxicity, leakage, and recycling of lead in perovskite photovoltaics. Adv Energy Mater, 2023, 13: 2204144
11 Ke W, Kanatzidis M G. Prospects for low-toxicity lead-free perovskite solar cells. Nat Commun, 2019, 10: 965
12 Li J, Cao H L, Jiao W B, et al. Biological impact of lead from halide perovskites reveals the risk of introducing a safe threshold. Nat Commun, 2020, 11: 310
13 Krishnamoorthy T, Ding H, Yan C, et al. Lead-free germanium iodide perovskite materials for photovoltaic applications. J Mater Chem A, 2015, 3: 23829–23832

14 Zhou J, Rong X, Molokeev M S, et al. Exploring the transposition effects on the electronic and optical properties of $Cs_2AgSbCl_6$ via a combined computational-experimental approach. J Mater Chem A, 2018, 6: 2346–2352

15 Saparov B, Hong F, Sun J P, et al. Thin-film preparation and characterization of $Cs_3Sb_2I_9$: a lead-free layered perovskite semiconductor. Chem Mater, 2015, 27: 5622–5632

16 Du J, Shi J. 2D $Ca_3Sn_2S_7$ chalcogenide perovskite: a graphene-like semiconductor with direct bandgap 0.5 eV and ultrahigh carrier mobility 6.7×10^4 cm^2 V^{-1} s^{-1}. Adv Mater, 2019, 31:

17 Shin J F, Xu W, Zanella M, et al. Self-assembled dynamic perovskite composite cathodes for intermediate temperature solid oxide fuel cells. Nat Energy, 2017, 2: 16214

18 Slavney A H, Smaha R W, Smith I C, et al. Chemical approaches to addressing the instability and toxicity of lead–halide perovskite absorbers. Inorg Chem, 2016, 56: 46–55

19 Gu S, Lin R, Han Q, et al. Tin and mixed lead–tin halide perovskite solar cells: progress and their application in tandem solar cells. Adv Mater, 2020, 32:

20 Fang H H, Adjokatse S, Shao S, et al. Long-lived hot-carrier light emission and large blue shift in formamidinium tin triiodide perovskites. Nat Commun, 2018, 9: 243

21 Hao F, Stoumpos C C, Cao D H, et al. Lead-free solid-state organic–inorganic halide perovskite solar cells. Nat Photon, 2014, 8: 489–494

22 Umari P, Mosconi E, de Angelis F. Relativistic GW calculations on $CH_3NH_3PbI_3$ and $CH_3NH_3SnI_3$ perovskites for solar cell applications. Sci Rep, 2014, 4: 4467

23 Yang W F, Igbari F, Lou Y H, et al. Tin halide perovskites: progress and challenges. Adv Energy Mater, 2020, 10:

24 Kamarudin M A, Hirotani D, Wang Z, et al. Suppression of charge carrier recombination in lead-free tin halide perovskite via lewis base post-treatment. J Phys Chem Lett, 2019, 10: 5277–5283

25 Awais M, Kirsch R L, Yeddu V, et al. Tin halide perovskites going forward: frost diagrams offer hints. ACS Mater Lett, 2021, 3: 299–307

26 Shockley W, Queisser H J. Detailed balance limit of efficiency of *p-n* junction solar cells. J Appl Phys, 1961, 32: 510–519

27 Rühle S. Tabulated values of the Shockley–Queisser limit for single junction solar cells. Sol Energy, 2016, 130: 139–147

28 Shi Y, Zhu Z, Miao D, et al. Interfacial dipoles boost open-circuit voltage of tin halide perovskite solar cells. ACS Energy Lett, 2024, 9: 1895–1897

29 Wu T, Liu X, Luo X, et al. Lead-free tin perovskite solar cells. Joule, 2021, 5: 863–886

30 Abdel-Shakour M, Chowdhury T H, Matsuishi K, et al. High-efficiency tin halide perovskite solar cells: the chemistry of tin (II) compounds and their interaction with lewis base additives during perovskite film formation. Sol RRL, 2021, 5: 2000606

31 Jokar E, Chien C H, Fathi A, et al. Slow surface passivation and crystal relaxation with additives to improve device performance and durability for tin-based perovskite solar cells. Energy Environ Sci, 2018, 11: 2353–2362

32 Wang C, Gu F, Bian Z, et al. Advances on tin-based perovskite solar cells. Chin Sci Bull, 2021, 66: 2129–2138

33 Xu P, Chen S, Xiang H J, et al. Influence of defects and synthesis conditions on the photovoltaic performance of perovskite semiconductor $CsSnI_3$. Chem Mater, 2014, 26: 6068–6072

34 Noel N K, Stranks S D, Abate A, et al. Lead-free organic–inorganic tin halide perovskites for photovoltaic applications. Energy Environ Sci, 2014, 7: 3061–3068

35 Jiang X, Zang Z, Zhou Y, et al. Tin halide perovskite solar cells: an emerging thin-film photovoltaic technology. Acc Mater Res, 2021, 2: 210–219

36 Goyal A, McKechnie S, Pashov D, et al. Origin of pronounced nonlinear band gap behavior in lead–tin hybrid perovskite alloys. Chem Mater, 2018, 30: 3920–3928

37 Xiao Z, Song Z, Yan Y. From lead halide perovskites to lead-free metal halide perovskites and perovskite derivatives. Adv Mater, 2019, 31: e1803792

38 Lee S J, Shin S S, Im J, et al. Reducing carrier density in formamidinium tin perovskites and its beneficial effects on stability and efficiency of perovskite solar Cells. ACS Energy Lett, 2017, 3: 46–53

39 Liu T, Troisi A. What makes fullerene acceptors special as electron acceptors in organic solar cells and how to replace them. Adv Mater, 2013, 25: 1038–1041

40 Liu K, Tian C, Liang Y, et al. Progress toward understanding the fullerene-related chemical interactions in perovskite solar cells. Nano Res, 2022, 15: 7139–7153

41 Lv S, Gao W, Liu Y, et al. Stability of Sn-Pb mixed organic–inorganic halide perovskite solar cells: progress, challenges, and perspectives. J Energy Chem, 2022, 65: 371–404

42 Wu T, Cui D, Liu X, et al. Additive engineering toward high-performance tin perovskite solar cells. Sol RRL, 2021, 5: 2100034

43 Pereyra C, Xie H, Lira-Cantu M. Additive engineering for stable halide perovskite solar cells. J Energy Chem, 2021, 60: 599–634

44 Dutt V G V, Akhil S, Singh R, et al. Year-long stability and near-unity photoluminescence quantum yield of $CsPbBr_3$ perovskite nanocrystals by benzoic acid post-treatment. J Phys Chem C, 2022, 126: 9502–9508

45 Zou S, Ren S, Jiang Y, et al. Efficient environment-friendly lead-free tin perovskite solar cells enabled by incorporating 4-fluorobenzylammonium iodide additives. Energy Environ Mater, 2023, 6: e12465

46 Meng X, Wang Y, Lin J, et al. Surface-controlled oriented growth of $FASnI_3$ crystals for efficient lead-free perovskite solar cells. Joule, 2020, 4: 902–912

47 Liu X, Wu T, Chen J Y, et al. Templated growth of $FASnI_3$ crystals for efficient tin perovskite solar cells. Energy Environ Sci, 2020, 13: 2896–2902

48 Chen Y F, Luo Z M, Chiang C H, et al. Multifunctional ionic fullerene additive for synergistic boundary and defect healing of tin perovskite to achieve high-efficiency solar cells. ACS Appl Mater Interfaces, 2022, 14: 46603–46614

49 Chen J, Tian C, Sun C, et al. Chlorofullerene $C_{60}Cl_6$ enables efficient and stable tin-based perovskite solar cells. Energy Environ Mater, 2024, 7: e12529

50 Choi J, Yang S J, Han S G, et al. Defect-stabilized tin-based perovskite solar cells enabled by multifunctional molecular additives. Chem Mater, 2023, 35: 1148–1158

51 Chen J, Luo J, Hou E, et al. Efficient tin-based perovskite solar cells with trans-isomeric fulleropyrrolidine additives. Nat Photon, 2024, 18: 464–470

52 Hou E, Chen J, Luo J, et al. Cross-linkable fullerene enables elastic and conductive grain boundaries for efficient and wearable tin-based perovskite solar cells. Angew Chem, 2024, 136: e202402775

53 Lian J, Lu B, Niu F, et al. Electron-transport materials in perovskite solar cells. Small Methods, 2018, 2:

54 Warby J, Zu F, Zeiske S, et al. Understanding performance limiting interfacial recombination in pin perovskite solar cells. Adv Energy Mater, 2022, 12: 2103567

55 Shao Y, Xiao Z, Bi C, et al. Origin and elimination of photocurrent hysteresis by fullerene passivation in $CH_3NH_3PbI_3$ planar heterojunction solar cells. Nat Commun, 2014, 5: 5784

56 Li B, Wu X, Zhang H, et al. Efficient and stable tin perovskite solar cells by pyridine-functionalized fullerene with reduced interfacial energy loss. Adv Funct Mater, 2022, 32: 2205870

57 Sun C, Zhang H, Cheng S, et al. Multidentate fullerenes enable tunable and robust interfacial bonding for efficient tin-based perovskite solar cells. Adv Mater, 2024, 36: 2410248

58 Wu C, Zhu W, Wang S, et al. Raising the LUMO level of fullerene derivatives alleviates the output voltage loss in tin halide perovskite solar cells. Chem Commun, 2022, 58: 13007–13010

59 Jiang X, Wang F, Wei Q, et al. Ultra-high open-circuit voltage of tin perovskite solar cells via an electron transporting layer design. Nat Commun, 2020, 11: 1245

60 Yu B B, Chen Z, Zhu Y, et al. Heterogeneous 2D/3D tin-halides perovskite solar cells with certified conversion efficiency breaking 14%. Adv Mater, 2021, 33: 2102055

61 Wang J, Yang C, Chen H, et al. Oriented attachment of tin halide perovskites for photovoltaic applications. ACS Energy Lett, 2023, 8: 1590–1596

62 Zhu Z, Jiang X, Yu D, et al. Smooth and compact $FASnI_3$ films for lead-free perovskite solar cells with over 14% efficiency. ACS Energy Lett, 2022, 7: 2079–2083

63 Sun C, Yang P, Nan Z, et al. Well-defined fullerene bisadducts enable high-performance tin-based perovskite solar cells. Adv Mater, 2023, 35: 2205603

64 Yang P, Sun C, Fu X, et al. Efficient tin-based perovskite solar cells enabled by precisely synthesized single-isomer fullerene bisadducts with regulated molecular packing. J Am Chem Soc, 2024, 146: 2494–2502

65 Liu W, Huang G, Chen C Y, et al. An open-cage bis[60]fulleroid as an electron transport material for tin halide perovskite solar cells. Chem Commun, 2024, 60: 2172–2175

Summary for “功能化富勒烯在锡基钙钛矿太阳能电池中的研究进展”

Research progress on functionalized fullerenes in tin-based perovskite cells

Chao Sun, Yiming Xing, Hui Zhang, Shanshan Chen, Chengbo Tian* & Zhanhua Wei*

Xiamen Key Laboratory of Optoelectronic Materials and Advanced Manufacturing, Institute of Luminescent Materials and Information Displays, College of Materials Science and Engineering, Huaqiao University, Xiamen 361021, China
* Corresponding authors, E-mail: cbtian@hqu.edu.cn; weizhanhua@hqu.edu.cn

In recent years, organic-inorganic halide perovskite solar cells (PSCs) have gained significant attention and experienced rapid advancements, thanks to their high light absorption coefficients, tunable bandgaps, low exciton binding energies, and solution processability. Within just over a decade, the power conversion efficiency (PCE) of PSCs has surged from 3.8% to 26.7%, positioning them as one of the leading technologies in the third generation of photovoltaics. However, the vast majority of high-efficiency PSCs currently rely on lead-based perovskite, raising concerns about the potential risks associated with lead leakage during production, transportation, storage, and usage, which could lead to biological hazards and environmental pollution. As a result, various low-toxicity or non-toxic lead-free perovskite materials have been developed in an attempt to replace the toxic lead-based compounds. Among these alternatives, tin-based perovskites (TPSCs) are considered promising. Tin, being in the same group as lead on the periodic table, shares similar atomic structures and ionic radii, enabling tin-based perovskites to exhibit many optoelectronic properties akin to lead-based perovskites, such as high carrier mobility and excellent light absorption coefficients. Additionally, tin-based perovskites possess a narrower bandgap, which approaches the theoretical optimal bandgap for single-junction solar cells (approximately 1.34 eV), potentially allowing TPSCs to achieve efficiencies exceeding 33%. However, the highest PCE of TPSCs to date is still only 15.7%, which is considerably lower than the theoretical efficiency.

Fullerenes, which are spherical conjugated π systems made up of multiple five-membered and six-membered rings, have emerged as a potential solution. These molecules exhibit high electron mobility, efficient defect passivation properties, and the ability to introduce various functional groups. As a result, fullerene derivatives with specific functionalities have been extensively used in TPSCs to address several of the challenges these devices face. Due to their excellent conductivity, various functionalized fullerenes have been incorporated into tin-based perovskite precursor solutions. Studies show that these large spherical fullerene additives tend to concentrate at the grain boundaries of the perovskite, where they function as carrier transport media between grains. Additionally, fullerenes can passivate grain boundary defects by interacting with Sn^{2+} ions, preventing their oxidation. Some cross-linkable fullerene additives have been employed to delay the crystallization process, optimize lattice matching, and reduce mechanical stress within the thin film, which not only improves device efficiency but also makes them suitable for applications in wearable devices. Another key strategy to improve the performance of TPSCs involves optimizing the interface between the perovskite and electron transport layers (ETLs). The common-used solvents for fullerene interface modification do not damage the underlying tin-based perovskite, and these fullerenes can also enhance interactions with the tin-based perovskite by introducing suitable functional groups, thereby improving electron extraction and defect passivation, which effectively enhances device performance. Furthermore, the development of fullerene materials with higher lowest unoccupied molecular orbital (LUMO) levels and stronger coordinating interactions for direct use as ETLs can help resolve energy-level mismatches in TPSCs. Research has shown that a series of fullerene bisadducts, which possess suitable LUMO levels and enhanced passivation effects, have been successfully employed in TPSCs, resulting in substantial performance improvements.

In conclusion, although there is still a noticeable PCE gap between TPSCs and lead-based perovskite solar cells (LPSCs), the promising theoretical efficiency and low toxicity of TPSCs highlight their commercial potential. Continued exploration of functionalized fullerene materials, along with ongoing advancements in device performance, will be key to unlocking the full capabilities of tin-based perovskites in photovoltaic energy generation.

tin-based perovskite solar cells, functionalized fullerenes, energy level matching, interface passivation, crystallization regulation

doi: 10.1360/TB-2024-1360